Thermoresponsive mucoadhesive hydrogel based on Pluronic F127/ thiolated glycol chitosan for intravesical administration of celecoxib/ gemcitabine

Fabrizio Ricci[1, #], Giuseppe Francesco Racaniello[2, #], Nunzio Denora[2], Luigi Gentile[3], Antonio Lopalco[2], Annalisa Cutrignelli[2], Massimo Franco[2], Rosa Maria Iacobazzi[2], Valentino Laquintana[2, *] Angela Lopedota[2, *]

[1]Department of Pharmaceutical Technology, University of Innsbruck, Institute of Pharmacy, Center for Chemistry and Biomedicine, Innsbruck, 6020, Austria

[2]Department of Pharmacy – Pharmaceutical Sciences, University of Bari "Aldo Moro", 70125 Bari, Italy

[3]Department of Chemisry - University of Bari "Aldo Moro", 70125 Bari, Italy

[#] These authors are the co-first name

* Corresponding author: valentino.laquintana@uniba.it; angelaassunta.lopedota@uniba.it;

ABSTRACT

In the last years, to improve the therapeutic outcomes of bladder cancer patients some mucoadhesive *in situ* gelling formulations for intravesical application have been studied. Here, we carefully tuned a Pluronic F127-based thermoresponsive gel using two mucoadhesive thiolated derivatives of glycol chitosan, S-preactivated N-acetylcysteine (NAC)- and glutathione (GSH)-glycol chitosan (GC). The gel was loaded with a combinational therapy of Gemcitabine (GEM) and Celecoxib (CEX), for this last aqueous solubility was increased for a synergic influence between Pluronic and inclusion complex of 2-Hydroxypropyl-β-cyclodextrin/CEX. The effect of the inclusion complex and of the two mucoadhesive polymers on rheological features of Pluronic based gels were highlighted to select the best. Finally, ex-vivo retention studies and in-vitro drug release of the selected systems were monitored for 24 h, providing enhanced retention properties (50% after 6h) and continued drug release.

KEYWORDS

Bladder cancer; Cyclodextrin; Gemcitabine; Celecoxib; Thermoresponsive Hydrogel; Thiomers; Hydrogel rheology.

1. INTRODUCTION

Bladder cancer (BC) is ninth cancer for incidence and the thirteenth cause of death among malignant diseases (Sanli et al., 2017). Urothelial cell carcinoma is the most common type of bladder cancer (BC) (Martins-Lima et al., 2023). When BC invades the detrusor muscle, it is regarded as muscle-invasive BC (MIBC) and it is more likely to metastasize to lymph nodes and other organs, otherwise it is regarded as non-muscle-invasive BC (NMIBC). MIBC and NMIBC have an incidence rate of 25% and 75%, respectively. Due to the absence of active screening and a cure for metastatic disease, mortality rates have not changed over the years (Ramirez et al., 2016). Hematuria, microscopic (invisible) or macroscopic (visible) blood in the urine, is the most common symptom of BC and usually associated with advanced non-muscle-invasive BC at the pathological stage.

After diagnosis, the current treatment for superficial NMIBC, except for carcinoma in situ (CIS), is transurethral resection of the bladder tumor (TURBT) followed by intravesical immunotherapy with Bacillus Calmette-Guerin (BCG), an attenuated strain of Mycobacterium Bovis used to decrease the risk of recurrence and slow progression. However, it has been demonstrated that more than 50% of patients will fail by not being disease free after one year from the treatment (van Rhijn et al., 2009). Owing to the high BC tumor heterogeneity, a single treatment cannot eradicate all cancer cells (Guo et al., 2020). Combination therapies can reduce the development of gene resistance and increase the effectiveness of the therapy. In many clinical trials, the combination of two anti-tumoral drugs reduced the recurrence rates at the 1 and 2 years follow, however this resulted in higher (17%) grade 3 toxicity.

Gemcitabine (GEM) (2,2-Difluordesoxycytidin), commercially known as Gemzar®, was approved by the FDA in 2004 as a second-line treatment for NMBC after TURBT in combination with cisplatin. Hayashi et al. recently demonstrated that the co-delivery of GEM and a selective inhibitor of COX-2, celecoxib (CEX), significantly heightened the antitumor response and decreased tumor growth in mice 28 days after administration (Hayashi et al., 2020).

Cell death induced by antitumor drugs can be immunologically silent and is defined as tolerogenic or immunogenic cell death (ICD). Anticancer therapeutics capable of inducing ICD can increase their efficacy by recruiting anti-tumor immunity (Galluzzi et al., 2017). These drugs can release host-derived immune-activating molecules known as damage-associated molecular patterns (DAMPs) from the dying cells. GEM cannot induce ICD because of the low levels of DAMPS expressed in the tumor environment after its administration. Moreover, prostaglandin 2 (PGE-2), which is overexpressed in tumor tissues, functions as a DAMPs inhibitor. CEX, which prevents PGE-2 formation, increases DAMPs levels after GEM administration, induces ICD, and significantly enhances the antitumor effect of the combination therapy.

CEX is also able to reduce the COX-2 effect on carcinogenesis, resulting in a reduction in tumor growth in different studies (Harris, 2007; Morita et al., 2012).

Nevertheless, several factors limit the oral bioavailability of drugs targeted to vesica: poorly vascularized urothelium, low aqueous solubility or low absorption such as CEX and GEM respectively , and degradation due to gastric acids and hepatic enzymes. An increase in the systemic drug dose to increase the resulting local concentration would increase the risk of adverse drug reactions and nonselective toxic effects on healthy tissues.

To address these shortcomings, the intravesical drug delivery system (IDD) approach, which involves the local instillation of one or multiple therapeutic agents through a catheter directly into the bladder, has been widely investigated. IDD has numerous advantages, such as site-specific drug delivery with minimal toxicity, the possibility of modulation of the administered dose, and the possibility of multiple administrations. Localized therapy improves therapeutic drug concentrations in the bladder and destroys residual urothelial cancer cells (Yoon et al., 2020). Owing to its low aqueous solubility (BCS class II drug), CEX was complexed with a semisynthetic derivative of native β-cyclodextrin (β-CD) and random-methyl-β-cyclodextrin (Rame-β-CD). After complexation, it was encapsulated in chitosan (CS) microparticles for intravesical administration with the aim to increase bladder retention time and proposed as alternative to CEX conventional oral formulation (Lopedota et al., 2016).

Nevertheless, IDD faces major drawbacks, such as periodic organ voiding by urine washing, risk of possible infections and inflammations due to frequent catheterizations, and unpleasant patient experiences. To increase the retention time of the drug on the bladder wall, IDD with increased mucoadhesive properties have been explored (Denora et al., 2016; Yoon et al., 2020). Often, IDD suggested for this route are gels, particularly thermoresponsive hydrogels. They are IDD systems with sol-gel transition properties in the physiological temperature range (32-37 °C), capable of prolonging drug dwell times in the bladder (Lin et al., 2014; Sherif et al., 2018). Specifically, it is required to remain in a 'free-flowing' sol state, with low viscosity at low temperatures, and maintain an 'injectable' state that helps in administration and spreading into the bladder. However, when the temperature is increased to physiological levels, they rapidly have to undergo a sol-gel transition and form a 'hard-to-flow' gel phase with high viscosity to prolong its retention on the bladder wall. A jellification polymer with this behavior is the Pluronic F127 (F127), a triblock copolymer composed of a central chain of polyoxypropylene and two side chains of polyoxiethylene (PEOn–PPOn–PEOn) (Gentile et al., 2010).

F127-based hydrogels exhibited very poor mucoadhesive properties once placed in the biological medium and many strategies such as chemical modifications in F127 gels can be attempted. Thus, chemically-modified F127 gels have been already described in the literature to obtain improved mucoadhesive and mechanical properties. Furthermore, physical strategies can be intended to reach acceptable mucoadhesive properties. Therefore,

mucoadhesive agents or polymers have been used in combination with F127 to improve these characteristics.

Recently, thiolated polymers, also known as thiomers, have been extensively explored to enhance the mucoadhesive properties of different polymers (Hock et al., 2022; Ricci et al., 2022). Thiomer can form covalent disulfide bonds with cysteine-rich subdomains of mucus within an oxidizing or alkaline environment, thus increasing the residence time onto mucosa, however, the high reactivity of the free thiol group leads to an instant reaction with the superficial thiol groups of the mucosa and an easy elimination by constant mucus renewal.

Second-generation thiomers, presenting thiol groups given by the presence of glutathione (GSH) or the cysteine and subsequently protected through interaction by biocompatible molecules, such as 2-mercapto-nicotinic acid (MNA) with the thiol group, were studied by our group obtaining numerous advantages: decreased reactivity, improved permeation properties, increased residence time in mucus, and stability toward oxidation during storage at higher pH (Perrone et al., 2018; Racaniello et al., 2021).

Indeed, two thiolated derivatives of Glycol Chitosan (GC), S-preactivated N-acetylcysteine (NAC)- and glutathione (GSH)-glycol chitosan (GC) (GC-NAC-MNA and GC-GSH-MNA, respectively) were synthesized and characterized (Perrone et al., 2018). The polymers displayed enhanced mucoadhesive properties in-vitro and ex-vivo compared to non-thiolated and non-protective precursors.

On these assumptions, the aim of this project was to produce a new thermoresponsive hydrogel formulation based on F127 with increased mucoadhesive properties by including the well-known mucoadhesive CS and the GC-NAC-MNA and the GC-GSH-MNA thiomers for the intravesical co-delivery of CEX and GEM suitable to treat BC. In these gels, CEX was added after complexation with hydroxypropyl-β-CD (Hp-β-CD) by freeze dried method. A systematic study regarding the amount of F127 and its ratio with the mucoadhesive polymers was conducted to optimize the sol-gel transition properties. After narrowing the list to the most promising, rheological and retention time studies were conducted. Finally, in-vitro release profiles of CEX and GEM from the most promising formulations were investigated.

2. MATERIALS AND METHODS

2.1. Materials

Low-viscosity chitosan (50 kDa MW), glycol chitosan (degree of polymerization > 400; GC), glutathione (GSH), N-acetylcysteine (NAC), 1-ethyl-3-(3-dimethylaminopropyl) carbodiimide hydrochloride (EDAC), N-hydroxysuccinimide (NHS), 2-mercaptonicotinic acid (2-MNA), 2-

amino-2-(hydroxymethyl)-1,3-propanediol (TRIS), sodium borohydride ($NaBH_4$), gemcitabine hydrochloride (GEM), celecoxib (CEX), acetic acid water solution (96%), fluorescein diacetate (FDA), 5,5′-dithio-bis (2-nitrobenzoic acid) (Ellman's reagent), and the components of the buffer preparation were purchased from Sigma-Aldrich. Hydroxypropyl-β-CD (Hp-β-CD) (degree of substitution 7.5) was kindly donated by Farmalabor (Canosa, Italia). Pluronic F127 (F127) was purchased from BASF (Hamburg, Germany). Dialysis tubing cellulose acetate membranes (molecular weight cut-off of 3.5 kDa) were purchased from Spectrum, Italy.

2.2. Quantitative analysis

CEX was quantified by high-performance liquid chromatography (HPLC) using a reverse phase C18 column (5 µm particle size; 4.6 × 250 mm, Agilent). A mixture (85/15 V/V) of methanol and water (HPLC grade) was used as the mobile phase, with a flow rate of 0.8 mL/min, 10 min run time, oven temperature of 25 °C, and detection wavelength of 251 nm. A linear calibration curve was obtained by dissolving 1 mg/mL of CEX in ethanol and through progressive dilutions, and a calibration curve was obtained in the range of 500–1 µg/mL (R^2 = 0.9996). The detection and quantification limits were 0.036 µg/mL and 1.0 µg/mL, respectively. GEM-HCl was quantified using a Hypersil (5 µm particle size; 4.6 × 150 mm), with a mobile phase consisting of ammonium acetate 1.0 mM and acetonitrile (97.5/2.5 V/V), with a flow of 0.7 mL/min, 10 min run time, oven temperature set at 25 °C, and detection wavelength set at 284 nm. A linear calibration curve was obtained by dissolving 1.0 mg/mL GEM-HCl in HPLC-grade water, and a calibration curve was obtained in the linearity range of 200–5 µg/mL) (R^2 =0.9999). The detection and quantification limits were 0.0156 µg/mL and 5 µg/mL, respectively.

2.3. Phase-solubility studies

The complexation constant $K_{1:1}$ between CEX and Hp-β-CD was studied and characterized according to Higuchi-Connors phase solubility studies (Higuchi-Connors, 1965) following a previously used protocol (Ricci et al., 2022). Aqueous solutions of Hp-β-CD were prepared at concentrations of 0, 1.25, 2.5, 5.0, 10, 20, 30 % (w/V). Excess amount of CEX was added to 5 mL of each solution in volumetric flasks. After stirring for 2 days at a controlled temperature of 13 °C, the suspensions were filtered through 0.45 µm cellulose acetate membrane syringe filters (Corning Syringe filters, Merck, Germany). An aliquot of the solution was withdrawn and the increased CEX water solubility due to CD complexation was quantified by HPLC.

2.4 Determination of the solubility of CEX in F127 and HP-β-CD solutions

Solutions were prepared at concentrations of 1, 2, 5, 10, 17 and 20 % w/V of F127. To 1 mL of each solution (set in 4-mL screw-top vials) an excess of CEX was added, and the vials were placed for 48 h in the orbital shaker (MaxQ 6000, Thermo Scientific, United States) at 13 °C. Subsequently, the suspensions were filtered through cellulose acetate membrane filters of 0.22 µm porosity and, after appropriate dilution, were analyzed by HPLC. Then, starting from solutions of F127 in the range of 17 to 20 % w/V, six new solutions were prepared by increasing the concentrations of Hp-β-CD (0.5, 1, 2 % w/V). In these final solutions, an excess of CEX was added and its solubility in each sample was studied as described above.

2.5 Synthesis and characterization of glycol chitosan S-preactivated with NAC or GSH

According to a previously described procedure (Perrone et al., 2018), S-preactivated thiolated GC derivatives were developed (**Figure 1**)**.** In brief, a hydrochloric acid-adjusted water solution of GC (pH 5.0) was dropped into a previously prepared solution containing NAC or GSH, NHS, and EDAC in the same medium (pH 5.0). The obtained polymer conjugates of GC-NAC and GC-CSH were further purified by centrifugation. The precipitated polymer was then washed with Milli-Q water and lyophilized under reduced pressure for 25 hours. The resulting GC-NAC and GC-GSH were further protected by a disulphide bond exchange reaction with 2-MNA dimer, which was previously obtained by oxidizing 2-MNA. The lyophilized conjugates were stored in a vacuum desiccator at 4 °C. Before studies, the modified polymers were easily hydrated in an aqueous solution, forming a solution with low viscosity.

To quantify the amount of free and bound thiol groups in the polymer, Ellman's test was conducted, as previously described (Perrone et al., 2018; Ricci et al., 2022). To calculate the amount of polymer-free thiol groups, NAC and GSH were used as the standards. Furthermore, to reduce the existing intra- and intermolecular disulfide bonds, the polymer solutions were treated with $NaBH_4$, and the number of thiol groups was determined photometrically using Ellman's reagent. The number of disulfide bonds was calculated by subtracting the quantity of free thiol groups from the total amount of thiol moieties present in the polymer.

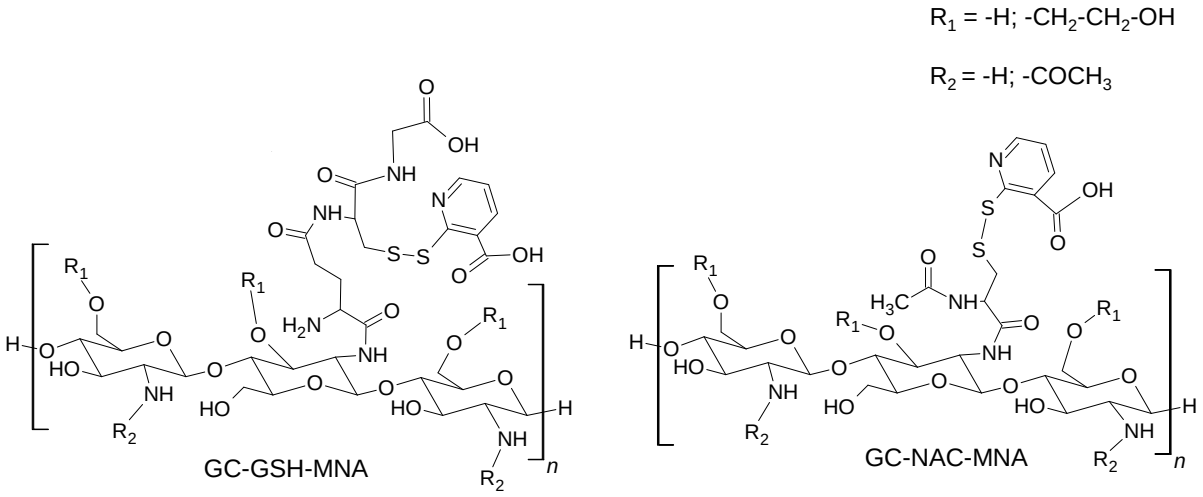

Figure 1. Representation of CG-GSH-MNA and GC-NAC-MNA

2.6. Screening study of excipients constituting the hydrogel

In order to find the best compromise between sol-gel temperature transition of F127 and ease of handling, especially syrengeability, a systematic study was conducted regarding 15 different combinations of excipients constituting the hydrogels. Specifically, the analyzed variables were the combination of F127 and mucoadhesive polymers (CS, GC-NAC-MNA, and GC-GSH-MNA) at different concentrations (% w/V). In all gels fixed amount of Hp-β-CD 2% (w/V) was used. The detail of the formulations are listed in **Table 1**. For the preparation, first, mucoadhesive polymers were dissolved in a 2 % (V/V) glacial acetic acid aqueous solution to increase the solubility of CS and preserve the unprotected free thiol groups of GC-GSH-MNA and GC-NAC-MNA. A 4 % (w/V) Hp-β-CD solution was prepared and diluted with equal volume of mucoadhesive polymer solutions to obtain the desired final concentrations, as shown in **Table 1** (pH values ranging between 3.50 and 4.60). The CS/Hp-β-CD, GC-GSH-MNA/Hp-β-CD, and GC-NAC-MNA/Hp-β-CD solutions were then used to solubilize exactly weighed amounts of F127 to obtain formulations coded as A1-A5 for CS based, B1–B5 for GC-NAC-MNA-based and C1-C5 for GC-GSH-MNA based, which were stored at 4 °C until further use.

Table 1. Screening study for the selection of excipients constituting the gel.

Code*	F127	CS	GC-NAC-MNA	GC-GSH-MNA

	A1	20	0.5	-	-
	A2	18	0.5	-	-
	A3	17	1.5	-	-
	A4	17	1	-	-
	A5	17	0.5	-	-
	B1	20	-	1	-
	B2	19	-	0.5	-
	B3	19	-	1	-
	B4	19	-	1.5	-
	B5	18	-	1.5	-
*All	**C1**	20	-	-	1
	C2	19	-	-	0.5
	C3	19	-	-	1
	C4	19	-	-	1.5
	C5	18	-	-	1.5

combinations have 2% w/v of HP-β-CD in a final solution of 1% (v/v) acetic acid

2.7. Gel characterization

2.7.1. Sol-gel transition temperature

Preliminary screening of the 15 combined formulations was adopted by evaluating their sol-gel transition temperature (Raghavan and Cipriano, 2006). Briefly, 5 mL of each formulation were poured into seal capped flasks and kept at 4 °C. The formulations were then immersed in a thermostated bath (Waterbath WTB, Memmert GmbH + Co.KG, Germany) at a temperature of 25 °C for a time of 5 min to simulate operating temperatures. Samples showing gelation at this temperature were discarded. The remaining samples were then immersed in a thermostated bath at a temperature of 37 °C for 5 min in order to evaluate their successful sol-gel transition at body temperature. Hence, the flasks were reversed upside - down and the effective gelation was visually evaluated, precisely when the visible flow was not observed within 30 s, the sample was regarded as a gel state.

2.7.2. Osmolarity and pH

The osmolarity of the formulations was measured using a manual Roebling osmometer (CamLab, Cambridge, UK) based on variations in the depression of freezing points. An amount of 100 µL of Double-distilled water or 0.9% w/V NaCl solution (used as a references) were poured into 1.5 mL Eppendorf tubes (Eppendorf, Hamburg, Germany). Once the calibration was performed (0 mOsm/L for the former and 300 mOsm/L for the latter), 100 µL

of each formulation was evaluated. The pH of the formulations was analyzed using a pHmeter (inoLab WTW labor level 1, France) after calibration with the standard solutions.

2.7.3. Syringeability studies

The syringeability of the remaining formulations was evaluated using a slightly modified piston-syringe method (Schuetz et al., 2008). In brief, 5 mL of each formulation, maintained at 4 °C, was poured into a syringe with a 21 Gauge diameter nozzle. The syringe was fixed to a vertical support using a clamp. A second clamp was fixed in the upper part, and a 1 kg weight was applied to the piston (**Figure 2**). The time, expressed in seconds, required to completely syringe the formulation (the lowest level of piston in the syringe) was estimated.

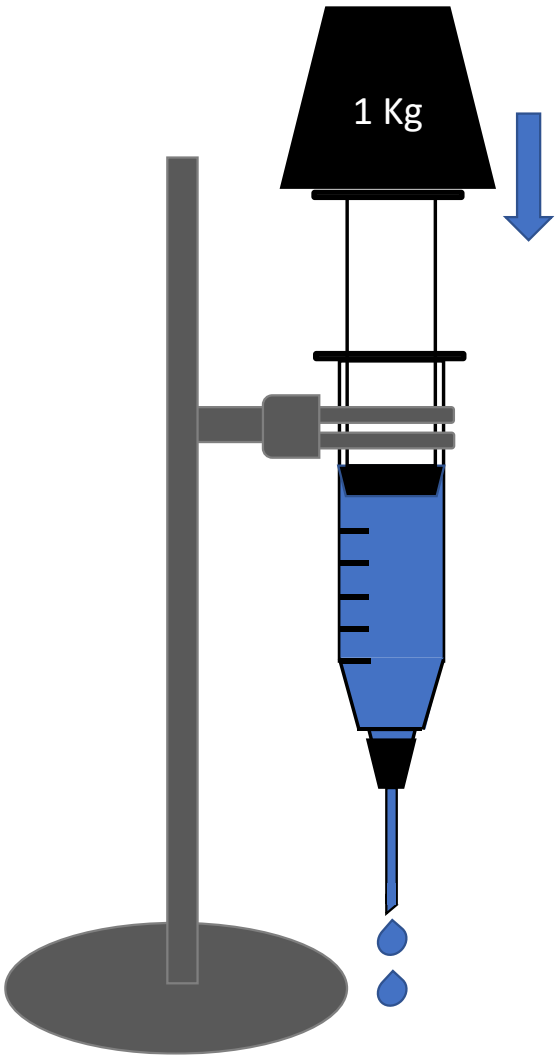

Figure 2. Analytical set up for syringeability evaluation.

2.7.4. Ex-vivo gel retention evaluation

To evaluate the total retention time of the A5, B4 and C4 on vesical mucosa ex-vivo retention time studies were performed using a previously described method (Racaniello et al., 2021). Freshly excised pig bladders were collected from the local slaughterhouse and placed in an ice bath. After careful washing, the bladders were cut into 4 × 3 cm pieces and stored at 4 °C until further use. Each gel formulation (5 mL) was loaded with 1 mg/mL of Fluorescein Diacetate (FDA). The formulations were applied to the mucosa as liquids and held horizontally at 37 °C to let gel formation. The piece of bladders was placed at an inclination of 45° in a thermostatic bath (37 ± 0.5 °C). 360 mL of phosphate buffer solution (PBS pH 6.8, 100 mM) flowing down the mucosa at 1 mL/min were collected in a falcon tube at several time points:0, 60, 120, 180, 240, 300 and 360 min. All the samples collected at different time points were vortexed for 30 s. To hydrolyze FDA to sodium fluorescein, 1 mL of 5 M NaOH was added to the equal amounts of each sample collected from the mucosa. The solutions were incubated for 20 min at 37 °C. The samples were then centrifuged using an Eppendorf Minispin at 13,400 rpm at room temperature for 5 min. Finally, 100 µL of each sample was transferred to a microplate to evaluate fluorescence intensity (λ_{Ex} = 485 nm and λ_{Em} = 535 nm).

Gel retention properties of each formulation at each time point were evaluated by measuring the % of retained gel still onto the mucosa and were expressed using equation (1):

$$Retention\ (\%) = 100 - \frac{Fluorescence\ (sample)}{Fluorescence\ \ (reference)} x100 \qquad \textit{(Eq. 1)}$$

A blank control was collected by rinsing the mucosa with only PBS (pH 6.8).

2.8. Gel loading and drug content assay

The formulations selected as performing better after the ex vivo retention evaluation test were loaded with GEM (0.5 % w/V) and CEX (0.12 %), as shown in **Table 2**. In detail, CEX (0.12% w/V) was added to a solution of 2% of HP-β-CD and mucoadhesive polymer. At these suspensions was added exactly weighed amounts of F127 (17 or 19% w/v) leaving the resulting suspension in stirring for 2 days at 13 °C, protected from light in order to have a complete solubilization of CEX. These medicated formulations (BL4 and CL4) were finally loaded with an exactly weighed amount of GEM (0.5%).

To assure the loading of two drugs into gels a previously described method was used (Sherif et al., 2018). Directly after preparation, 1 mL of each formulation was diluted into 100 mL of

double-distilled water in a volumetric flask. The amount of CEX and GEM was analyzed by HPLC.

Table 2. Composition of medicated gels.

Code	F127 %	CS %	GC-NAC-MNA %	GC-GSH-MNA %	Hp-β-CD %	CEX %	GEM %
BL4	19	-	1.5	-	2	0.12	0.5
CL4	19	-	-	1.5	2	0.12	0.5

2.9. Rheological evaluation

The temperature-induced sol-gel transition of the formulations BL4 and CL4 compared with the preparations B4, C4 (without Hp-β-CD) and F127 19% w/v was investigated using an Anton Paar MCR302e stress-controlled rheometer (Anton Paar Gmbh, Graz, Austria) equipped with a Taylor-Couette geometry, that is, a concentric cylinder geometry (inner diameter of 16.662 mm and gap of 0.704 mm), while the temperature was controlled by a Peltier system. The dynamic oscillatory shear experiments as a function of temperature (temperature sweep tests) were performed at a rate of 1°C/min from 15 °C to 55 °C in the linear viscoelastic regime, fixing the strain amplitude at 0.1% and the angular frequency at 10 rad/s to obtain the elastic G' and the viscous G'' moduli as a function of temperature. The onset of the sol-gel transition was considered to be the crossover between G' and G''. Furthermore, to evaluate the adhesive properties at 37 °C, a frequency sweep test (Gentile and Amin, 2022) was performed on selected samples in the linear viscoelastic regime (strain 0.1%).

2.10. *In-vitro* release studies

The in-vitro release profiles of CEX and GEM from BL4 and CL4 were investigated. Briefly, 4 mL of the formulation loaded with 20 mg of GEM-HCl and 4.8 mg of CEX were placed in a dialysis membrane tube (Spectra/Por regenerated cellulose, molecular weight cutoff 3.5 kDa). The dialysis membrane tubes were placed in 100 mL of PBS (pH 6.8, 100 mM) with 2% (w/V) of Hp-β-CD to assure sink conditions and stirred at 300 rpm at 37 °C. At predetermined time intervals of 0, 15, 30, 60, 120, 180, 240, 300, 360, 420, 480 and 1440 min, 2 mL aliquots were withdrawn and replaced with fresh medium. The aliquots thus collected were analyzed using the same HPLC method previously described, to estimate the drug content in the acceptor medium.

Then, the kinetics of drug release from the gel matrix was studied by employing various mathematical models using the following equations:

Zero-order kinetics equation (2):

$$\frac{M_t}{M_\infty} = kt \quad (Eq.2)$$

First-order kinetics equation (3):

$$\ln\left(\frac{M_t}{M_\infty}\right) = kt \quad (Eq.3)$$

The Peppas or Korsmeyer-Peppas kinetics equation (4):

$$\frac{M_t}{M_\infty} = kt^n \quad (Eq.4)$$

Higuchi equation (5):

$$\frac{M_t}{M_\infty} = kt^{1/2} \quad (Eq.5)$$

where M_t is the total amount of drug released at a time t, M_∞ is the total amount of drug cargo to be released, (Caccavo, 2019).

2.11. Statistical Analysis

The results are expressed as mean ± SD from three independent experiments. For retention mucoadhesive studies on bladder pig mucosa, statistical significance was calculated using two-way analysis of variance (ANOVA) followed by Brown-Forsythe test (GraphPad Prism version 5.0).

3. RESULTS AND DISCUSSIONS

Here are prepared new thermoresponsive hydrogels based on pluronic F127. New mucoahesive polymers (CS, GC-NAC-MNA and GC-GSH-MNA), were added to the formulations to obtain an in situ vesical gel able to prolong the residence onto mucosa of the organ permitting a co-deliver of CEX and GEM, selected drugs in this study to treat bladder cancer.

3.1 CEX/Hp-β-CD inclusion complex characterization

Natural CD and their semi-synthetic derivatives are used in different areas of drug delivery, especially for their well-known effects on drug solubility and dissolution, bioavailability, safety, and stability. Chemically modified CD derivatives have been prepared with a view to extending the physicochemical properties and inclusion capacity of parent CDs.

The degree of substitution (DS) indicates the number of substituents on the semisynthetic derivative starting from the native CD. Malanga et al. demonstrated how DS can influence host-guest complex formation and the solubilizing properties of oligosaccharides(Malanga et al., 2016). For this reason, despite the CEX/Hp-β-CD complex has been previously investigated, (Mennini et al., 2012; Ramaiah Chowdary and Srinivas, 2006; Sinha et al., 2011) phase-solubility studies according to Higuchi and Connors method were carried out to study the influence of the Hp-β-CD (DS=7.5) and temperature 13°C . This temperature was chosen to permit to have a liquid state when F127 was added in the next step of the study. The results of the phase solubility studies of CEX and Hp-β-CD at 13°C are shown in **Figure 3**. The complex displayed good linearity (R^2=0.9988) with an AL-type relationship and a 1:1 molar ratio inclusion complex between CEX and Hp-β-CD, according to the slope value (<1). The complex displayed a $K_{1:1}$ of 1508 M^{-1}, calculated using equation (6), indicating good stability of the formed complex (Pistone et al., 2022).

$$K_{1:1} = \frac{Slope}{S_0(1-Slope)} \qquad (Eq.\ 6)$$

Sinha et al. calculated $K_{1:1}$ values of 747 M^{-1} and 601 M^{-1} at 25 °C and 37 °C for the CEX/Hp-β-CD complex, respectively (Sinha et al., 2011); however, the DS of the utilized Hp-β-CD was not stated in the article. Nagarsenker et al. found a $K_{1:1}$ of 895 M^{-1} using Hp-β-CD with a DS of 4.9 after complexation at 30 °C (Nagarsenker and Joshi, 2005). Usually, the stability constant is inversely proportional to temperature because of the decrease in interaction forces, such as the van der Waals interaction energy and hydrophobic forces between the guest and host molecules (Beneš et al., 2012).

The intrinsic aqueous solubility of CEX is 0.036 mM (0.013.72 mg/ml) and, due to the CD complexation at maximum concentration evaluated in this study 30% (w/V), it increased to 1.190 mM with a 330-fold increment in solubility. In detail, at 2% (w/V) of CD, concentration used in the next step of this study, achieved a 35-fold increment in CEX aqueous solubility (0.48 mg/ml).

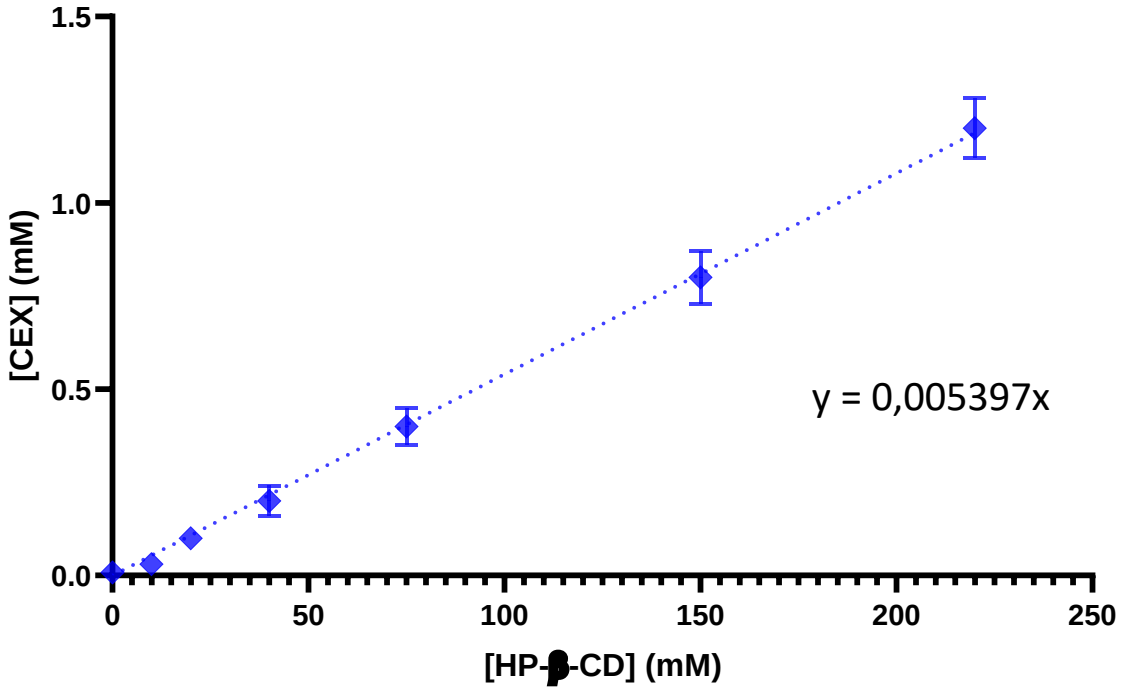

Figure 3. Phase solubility studies of CEX/Hp-β-CD inclusion complexes at 13 °C. Data are shown as mean ± SD (n=3).

A more precise parameter for evaluating the solubilizing effects of cyclodextrin is the efficiency of complexity (CE) (Lopedota et al., 2016)(Loftsson et al., 1999). It is the concentration ratio of cyclodextrin in a complex to free cyclodextrin. CE was calculated from the slope of the phase solubility diagram and is independent of both S_0 and the intercept. For a complex consisting of the drug and CD in the molar ratio 1:1, the CE is calculated as follows (Eq.7):

$$CE = S_0 \, x \, K_{1:1} = \frac{Slope}{1 - Slope} \quad (Eq. 7)$$

CE = 0.00542

Then the molar drug/CD ratio in the complexing medium can be calculated from the obtained CE value with the following formula (Eq.8):

$$Drug : CD = 1 : 1 + \frac{1}{CE} \quad (Eq. 8)$$

According to this equation, the calculated molar ratio for CB to HP-β-CD results in 1:185.

3.2 Characterization of mucoadhesive polymers

The lyophilized GC-GSH-MNA and GC-NAC-2MNA conjugates appeared as a white yellow powder with a fibrous structure and were odorless and sparingly soluble in aqueous solution. The amount of the attached thiol groups to the polymers was determinate by the Ellman's test, which demonstrated that on average 3.7 and 6.3 mmol of immobilized free thiol groups per gram of GC-GSH-MNA and GC-NAC-MNA conjugates, respectively. The obtained data showed a high percentage of disulfide bonds (0.4 and 1.2 mmol of oxidized thiol groups per gram of GC-GSH-MNA and GC-NAC-MNA conjugates, respectively), demonstrating a high percentage of protection (Perrone et al., 2017).

3.3 Screening study of excipients constituting the hydrogel

3.3.1 Sol-gel temperature transition screening

A preliminary screening of the sol-gel temperature transition properties of different combination of F127 and the CS, GC-GSH-MNA and GC-NAC-MNA, at fixed concentration of Hp-β-CD (Table 1), was carried out to discard those that were unable to form a gel over 37 °C. The investigated concentrations of F127 were above 15 (w/V), as the optimum F127 concentration range for aqueous gel IDD is between 17 -20% w/V, since they were proven to undergo a reversible thermal transition from easy handle micellar liquid to shear thinning phycal gels (Shriky et al., 2020).

Albeit, the presence of other substances in the preparation could change the gelling temperature. For example, CDs, when in the presence of F127 can form supramolecular structures that go to alter the pattern of gel formation (Simões et al., 2012). In addition, the use of CS at different concentrations (1-2 %) can significantly change the gelation temperature affecting them by ± 5 °C (Sherif et al., 2018). These results highlight the importance of understanding the effects of each component on gelation process.

As shown in **Table 3**, in the investigated samples, F127 at different concentrations in the presence of Hp-β-CD and mucoadhesive polymers appeared liquid at 25°C and gelled at 37°C, except in the case of samples B5 and C5. In this study, CS was tested in a concentration range up to 1.5% (w/V), higher values would increase the hydrogel viscosity at low temperatures and therefore affect the handling feasibility. How is possible to notice in **Table 3**, the CS presence in concentration as low as a 0.5% (w/V), with F127 concentration fixed at 17% (w/V), was sufficient to provide sol-gel transition properties in a temperature of 37 °C.

Despite increasing the mucoadhesive polymers and F127 concentrations up to 1.5% (w/V) and 18% (w/v), respectively in formulations B5 and C5, no sol-gel transition occurred at 37 °C and therefore were discarded. When the F127 concentration was raised to 19 or 20% (w/V), formulations B1-B4 and C1-C4, the sol gel transition occurred independently from GC-GSH-MNA or GC-NAC-MNA concentrations. Hence, at high concentrations of F127, the presence

of the polymers GC-GSH-MNA or GC-NAC-MNA has limited influence on the transition temperature of the formulations. Therefore, a higher concentration of F127 was used in the investigated formulations in order to ensure the sol-gel transition under physiological conditions while maintaining the equal concentration of mucoadhesive polymers.

3.3.2 Osmolarity and pH

As shown in **Table 3,** the osmolarity values of the formulations explored in this study, ranging from 377 to 543 mOsm/L, were within the tolerance range for the physiological conditions. The pH of the various formulations (ranging from 3.42 to 4.42) was measured to ensure that it was in the tolerance range for bladder in situ delivery (Tutak and Findikli, 2021) where the common value for urine pH is 6.0–7.5 but any value within the 4.5–8.0 range is generally not a cause for concern. Moreover, acid pH increases the ion permeability of the urothelium (Ifshin et al., 1983).

3.3.3 Syringeability studies

Syringeability, the ability of an IDD to be easily administered with a syringe and catheter, is an important factor to consider when developing a IDD (Şenyiğit et al., 2015). Jones et al. demonstrated that higher values of product viscosity corresponded to higher values of compression forces required for complete expulsion from the syringe (Jones et al., 1997). The nature and the concentration of the polymers included in the formulations can affect the viscosity, that should be kept as low as possible at room temperature for easier handling.

It is known that concentrations between 18–28% for F127 combine syringeability and in situ gelling, but the presence of other substances can change rheological characteristics of final preparation and consequential its syringeability. CS formulations are usually high-viscous formulations and are associated with difficulty handling and increased product loss due to adherence to the catheter wall (Schuetz et al., 2008). Compared to CS, GC in aqueous formulations exhibits lower viscosity values, increasing the administration feasibility (Cho et al., 2016). Therefore, syringeability studies were performed to find the right compromise between the sol-gel temperature transition properties and the viscosity of sol formulations during the administration by catheter.

The analyzed samples show a distinctive viscoelastic response . This characteristic can lead to a variation in the syringeability results obtained depending on the imparted strength and acceleration on the piston, which can lead to a response in the viscous modulus, thus with slow leakage of the solution, or in the elastic modulus, thus with blockage of the leakage. For this reason, all samples tested were treated by imparting exactly the same strength and acceleration, keeping only time as the testing determinant value (Alonso et al., 2021). As shown in **Table 3**, owing to its intrinsically high viscosity, the presence in formulations A1-A5 heavily affected their syringeability properties, requiring more time for complete leakage. During sample analysis, a partial gelation of formulation A3 in the syringe was evaluated and

therefore it was discarded. Due to the presence of GC derivatives, formulations B1-B4 and C1-C4 exhibited lower viscosities and therefore required lower times for complete leakage, ranging between 21 and 48 s.

Based on the overall results, formulation A5, B4 and C4 were selected as potential IDD because it provided the best compromise between good handling feasibility and gelling temperature.

Table 3. Sol-gel transition properties at 37 °C, pH, Osmolarity , and syringeability of the examined formulations.

Code	Gelation (37 °C)	pH	mOsm/l	Syringeability* (s)
A1	Yes	4.34	497	715 ± 17
A2	Yes	4.42	476	677 ± 48
A3	Yes	4.17	543	-
A4	Yes	4.21	484	662 ± 29
A5	Yes	4.16	453	113 ± 5
B1	Yes	3.42	423	45 ± 5
B2	Yes	3.50	377	22 ± 1
B3	Yes	3.44	401	33 ± 4
B4	Yes	3.82	394	39 ± 4
B5	No	-	-	-
C1	Yes	3.61	412	49 ± 8
C2	Yes	3.77	390	26 ± 3
C3	Yes	3.54	423	33 ± 2
C4	Yes	3.69	379	36 ± 3
C5	No	-	-	-

***** Syringeability of the formulations is expressed as second (s) required for a complete elution of 5 ml of preparation at 4°C.

3.4 *Ex-vivo* retention time evaluation

To evaluate the retention times of the selected formulations A5, B4 and C4, ex-vivo retention time evaluation was performed on pig bladder mucosa using FDA as tracer (**Figure 6A**). The results, shown in **Figure 6B**, were expressed as % of retained gel, calculated by difference of the initially % FDA into the gel and the amount of FDA registered from leakage after progressive washing with PBS.

Overall, gel B4 (CG-NAC-MNA based) provided the highest retention on the bladder mucosa throughout the analysis. In fact, after two hours from instillation, B4 was able to provide a

1.3-folder improvement in the retention of the gel compared to gel C4 and A5**.** Indeed, at this time, 94% of the initial amount was on the mucosa, value significantly different ($p < 0.05$) if compared to 75% for C4 (GC-GSH-MNA based) and 67% for the A5 (CS based).

Several factors have to be computed when the retention properties of different semi-solid formulations are evaluated: strength of ionic and covalent interactions between the formulation and the mucosa, mucus permeation properties, resistance to erosion and excessive hydration that may dilute the functional groups interacting with the biological membrane (Baus et al., 2019).

Furthermore, F127-based hydrogels based, due to its rapid disruption in the aqueous media, provide a drug release for a short period of time. One of the strategies we adopted to overcome this shortcoming is to modify the formulations by physically mixing it with other polymers as CS, or glycol chitosan derivates (GC-NAC-MNA, GC-GSH-MNA) that could modulate the F127 release profile based on in situ gelation system.

The increased mucoadhesion registered for B4 and C4, compared to the A5, is justified by the presence of the S-protected thiol groups. In fact, S-preactivated thiolated polymers show increased reactivity due to cross-linking from thiol group exchange reactions with mucin, providing longer residence time on mucous membranes and prolonged drug release at the target site (Racaniello et al., 2021). Furthermore, based on theoretical considerations, preactivated thiomers are even more reactive then first generation thiomers (Hock et al., 2022). The higher number of thiol groups present in the GC-NAC-MNA of gel B4 (6.3 mmol per g) respect GC-GSH-MNA of gel C4 should provide a higher interaction with the cysteine rich subdomains of the mucus, how demonstrated by previous studies conducted on these polymers (Perrone et al., 2018).

However, for a long retention of gel onto mucosa vesical other parameters had better to considerate as its susceptibility to urine erosion (Sherif et al., 2018) for this reason rheological study in deep was conducted on medicated BL4 and CL4 to further characterize them.

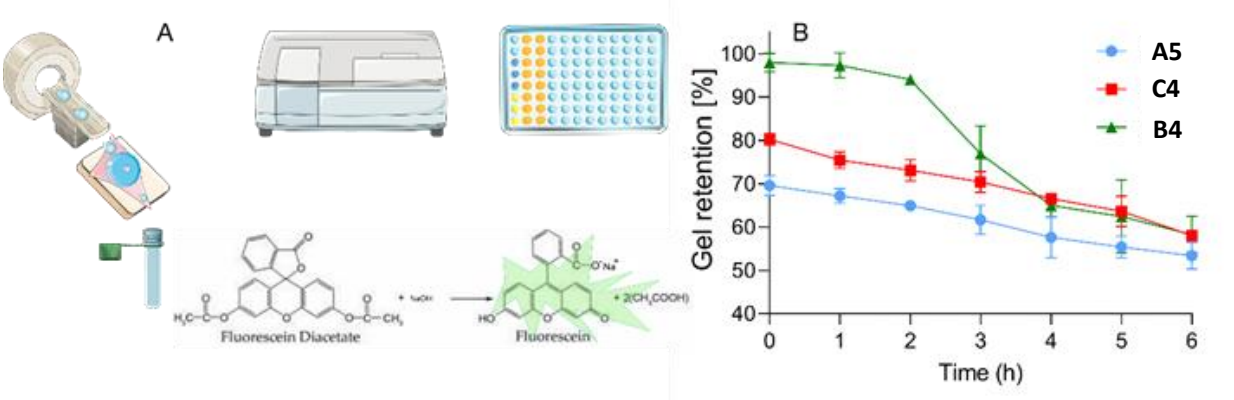

Figure 4. Ex-vivo retention time studies of tested formulations. **(A)** Analytical setup with PBS flushed over a gel attached to the mucosa and held at 45°. FDA was hydrolyzed with NaOH to its fluorescent derivative fluorescein sodium salt. **(B)** % of gel retention on the mucosa over time for tested formulations. Results are shown as mean ± SD (n=3).

3.5 Rheological evaluation

The gelation process of F127 has been widely investigated in the literature (Alexandridis and Alan Hatton, 1995; Gentile et al., 2010), and it is due to the formation of a micellar cubic phase. Below the gelation point, F127 exhibited only an isotropic phase composed of polymeric micelles. F127 is widely used in the pharmaceutical field owing to its stable gel phase at body temperature (Bodratti and Alexandridis, 2011; Bodratti and Alexandridis, 2018; Vinogradov et al., 2002).

Notably, after preparation, acetic acid was allowed to evaporate in all samples; in fact, the presence of acetic acid influenced the gelation process. An oscillatory temperature scan sweep showing G’ and G’’ as a function of temperature, **Figure 5** shows a shift in the gelation temperature, considered here as the G’-G’’ crossover. In particular, the gelation temperature shifted from 35 °C for F127 alone to ~ 28 °C for the systems in which GC-NAC-MNA and GC-GSH-MNA were introduced. Furthermore, the presence of the inclusion complex affects the gelation process; in fact, in the gel phase, G’ increases for BL4 with respect to the system free of the inclusion complex, whereas it decreases for CL4.

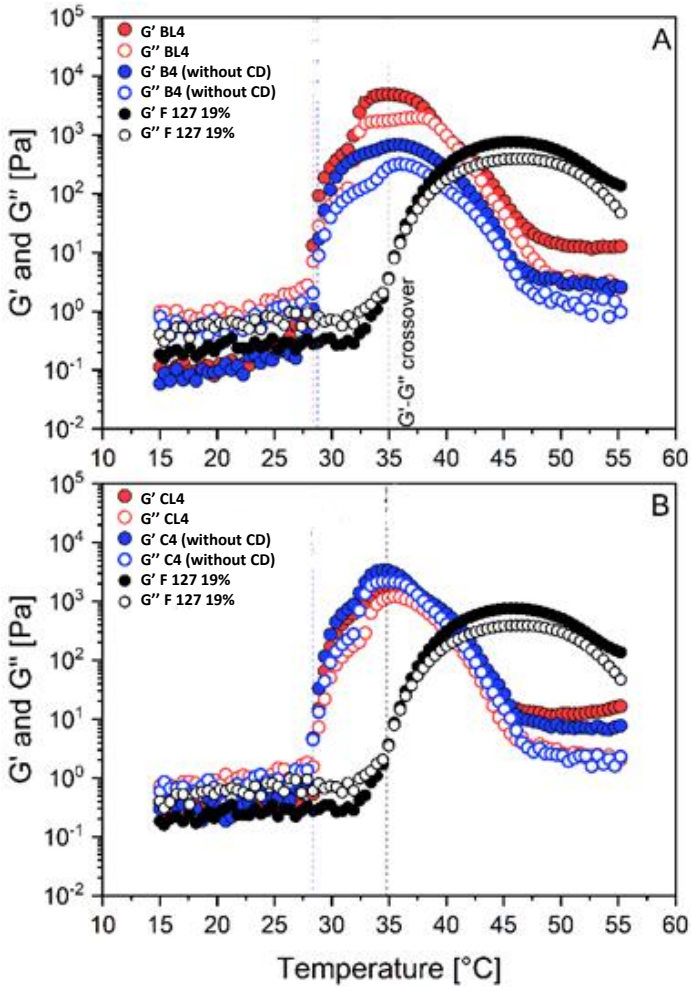

Figure 5. An oscillatory temperature scan was performed in the viscoelastic regime, reporting the elastic modulus, G', and the viscous modulus, G', as a function of temperature for F127; the corresponding system was modified by introducing GC-NAC-MNA (A) and GC-GSH-MNA (B)

The frequency dependence of the elastic modulus, G', at high frequency, was fitted to a general power law expression to evaluate the adhesive properties of the gel phase

$$G' = k\omega^n \qquad (Eq. 9)$$

where ω is the angular frequency, k the oscillatory consistency, and n the oscillatory exponent.

As shown in **Figure 5**, the frequency sweep at 37°C indicated that the presence of both GC-NAC-MNA and GC-GSH-MNA strongly affected the gel phase. The response of the moduli to increasing oscillatory frequency is a plateau region for F127, whereas a G'–G'' crossover, that is, a strong frequency dependency, is observable for the F127/GC-NAC-MNA and F127/GC-

GSH-MNA systems. **Table 4** reports the relaxation time τ as the inverse of the crossover frequency (Gentile and Amin, 2022), and k and n in eq.1.

Table 4. The oscillatory consistency and exponent k, and n, were obtained by fitting the data in Figure 5 at high frequency using equation (9), and the relaxation time, τ, was taken as the inverse of the G'-G'' crossover.

SAMPLE	τ (s)	k	n
G' F127 19%	-	688	0.032
B4 (without CD)	0.04	66	0.554
BL4	0.84	2469	0.166
C4 (without CD)	0.24	1223	0.259
CL4	0.10	242	0.454

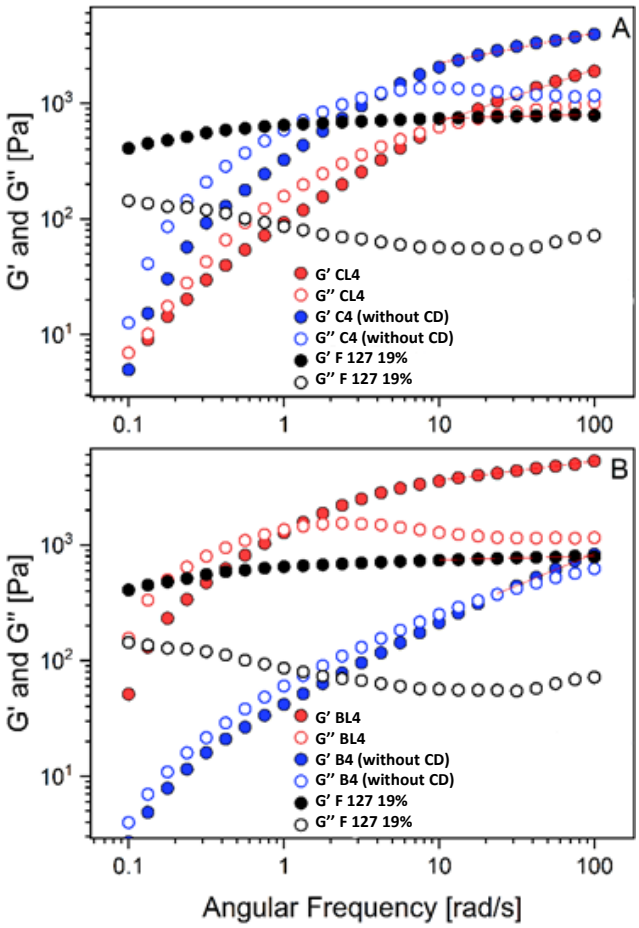

Figure 6. Frequency sweep experiments in the viscoelastic regime reported the elastic modulus, G', and the viscous modulus, G', as a function of the angular frequency for F127.

The corresponding system was modified by introducing GC-GSH-MNA (A) and GC-NAC-MNA (B) and the systems containing the inclusion complex. The red lines indicated the data fitting using equation (9)

The longer relaxation time for the BL4 with respect to all other investigated systems demonstrated increasing associativity between the polymers and the inclusion complex, whereas there was a lower association between GC-NAC-MNA and F127 in the absence of the inclusion complex with respect to GC-GSH-MNA (**Table 4**).

Significant increases in the oscillatory exponent (n) were observed in the presence of mucoadhesive polymers and upon addition of the inclusion complex for GC-GSH-MNA. Moreover, the oscillatory consistency of the BL4 was the heist among all the investigated samples. The oscillatory consistency was affected by the addition of the inclusion complex and choice of mucoadhesive polymer. CL4 resulted in the best adhesive system, whereas the more stable system was provided by BL4.

Therefore, the increased residence of gel BL4 onto mucosa may not only be attributed to its interactions with the mucus, but also to its higher stability and resistance towards erosion of gel that does not lack its mechanical strength in presence of liquid. Given the results of the rheological and of retention time studies, formulation BL4 was selected as the most promising formulation and further characterized in terms of its in-vitro release profile.

3.6 *In-vitro* release studies

The release profiles of GEM and CEX from the most promising formulation BL4 are shown in **Figure 7**. As it's possible to notice, both drugs displayed a continued release over time, with CEX released at a lower content (15%) compared to GEM (90%) over the 6 hours of analysis. The hydrogel nature of the formulation prevented a burst release of both drugs, protecting them for an extended period from the wash-out effect of the urine, presumably increasing their retention time in in-vivo conditions. The lower total release of CEX compared to GEM could be attributed to the drug-CD complex interaction that would represent an additional slowing factor, while GEM is directly dissolved in the aqueous phase of the gel (Sherif et al., 2018).

Furthermore, it was adopted empirical mathematical model that relates the amount of drug released and time. The use of different mathematical models is justified by the plethora of mechanisms affecting the release of the loaded drug: gel erosion, swelling properties and, as in this case, additional interactions with gel components as for the CD/CEX complex. Through experimental data by fitting to mathematical model it was possible to explain mechanisms that influenced the release of drugs CX and GEM from hydrogel matrix under study. In our work, five different kinetic models were used to identify the release mechanisms of CEX and GEM from the hydrogel.

The erosion effect of the aqueous medium can be explained by a rapid decomposition of the F127 micellar structure. The aqueous medium is able to dissolve the micelles on the surface, decomposing the gel and leading to a fast release of the drug. However, by modulating the mechanical strength of the gel by introducing other components, the erosion effect provided by the aqueous medium can be limited. The high correlation with the Korsemeyer-Peppas kinetics equation, shown in **Table 5**, expressed by both drugs, implies that the hydrogel was not subjected to major swelling or erosion phenomena during the analysis, suggesting the resistance of the formulation as already established in the rheological and retention studies. The GEM release from formulation B4 is better represented by a Korsmeyer-Peppas release kinetic. The identified n value (1.367) indicates that we are in the presence of a kinetic model of Super Case II type, characterized by an initial swelling phase of the outer layer of the gel and a subsequent release phase given by polymer chains breakdown, leading to a slowdown in drug release (Ahmed et al., 2019). On the other hand, a zero order kinetic

mathematical model was able to better fit the CEX release profile, indicating a constant release of the drug only as a function of time, independent of the concentration of the loaded actives (Bruschi, 2015). In addition, the system also displays a fitting with Korsmeyer-Peppas kinetics, and the shown n value (0.869) indicates that we are in the presence of an anomalous non-Fickian model, so the mechanism of drug release is governed by diffusion processes and polymeric swelling (Ahmed et al., 2019). Due to its prolonged release and retention in the bladder, the **BL4** formulation could increase the dwell time for both loaded drugs, extending the antitumor effect of dual administration.

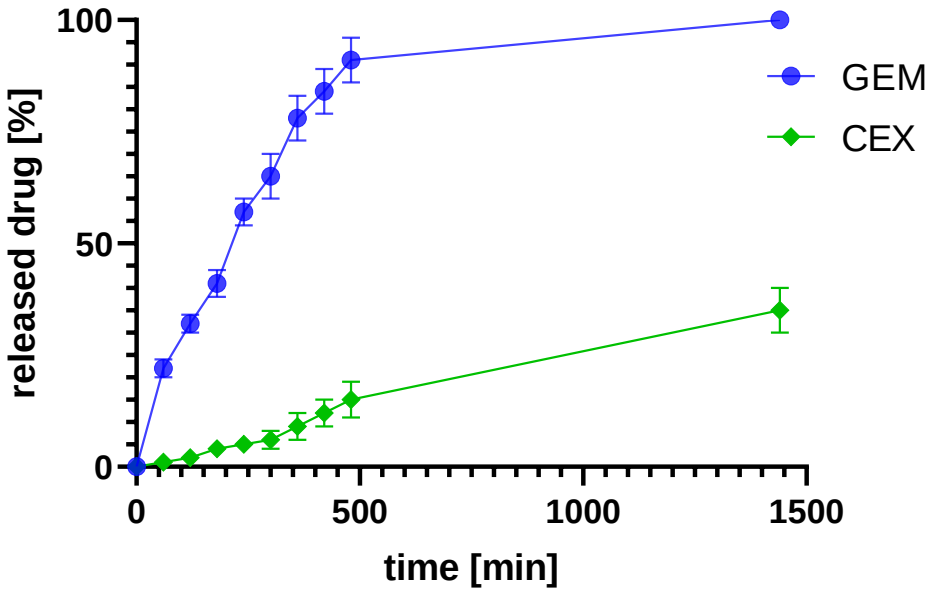

Figure 7. The in-vitro release profiles of GEM and CEX from the most promising formulation (B4) in PBS at pH 6.8. Results are shown as mean ± SD (n=3).

Table 5. Mathematical models applied to study the release kinetics of CEX and GEM from formulation **B4**.

Mathematical model	**CEX**		**GEM**	
	R^2	n	R^2	n
Zero order	0.9904		0.9927	
First order	0.9899		0.9654	
Higuchi	0.9552		0.9884	
Korsmeyer-Peppas	0.9810	0.833	0.9997	1.367

4 CONCLUSIONS

The main objective of this work is to develop a F 127 based thermosensitive hydrogel containing S-protected derivatives of glycol chitosan, in order to improve the mucoadhesive properties of the formulation, and HP-β-CD/CEX complex for enhancing the drug solubility. F127 provides sol-gel transition properties under physiological conditions, with transition temperatures varying in the presence of co-solutes. The *ex-vivo* retention time evaluation and rheological assays highlighted that GC-NAC-MNA provided the highest mucoadhesive properties, improving formulation residence time after bladder instillation. The *in-vitro* release profiles showed a controlled release of CEX and GEM up to 6h, providing a promising formulation for intravesical therapy of NMIBC.

Acknowledgments

The authors thank Siciliani SPA (Palo, (BA), Italy) for pig bladders. The authors gratefully acknowledge the University of Bari (Italy).

Conflict of interest

The authors declare that they have no conflict of interest.

REFERENCES

Alonso, J.M., Andrade del Olmo, J., Perez Gonzalez, R., Saez-Martinez, V., 2021. Injectable Hydrogels: From Laboratory to Industrialization. Polymers (Basel). https://doi.org/10.3390/polym13040650

Baus, R.A., Zahir-Jouzdani, F., Dünnhaupt, S., Atyabi, F., Bernkop-Schnürch, A., 2019. Mucoadhesive hydrogels for buccal drug delivery: In vitro-in vivo correlation study. European Journal of Pharmaceutics and Biopharmaceutics 142, 498–505. https://doi.org/10.1016/j.ejpb.2019.07.019

Caccavo, D., 2019. An overview on the mathematical modeling of hydrogels' behavior for drug delivery systems. Int J Pharm 560, 175–190. https://doi.org/10.1016/j.ijpharm.2019.01.076

Cho, I.S., Park, C.G., Huh, B.K., Cho, M.O., Khatun, Z., Li, Z., Kang, S.W., Choy, Y. bin, Huh, K.M., 2016. Thermosensitive hexanoyl glycol chitosan-based ocular delivery system for glaucoma therapy. Acta Biomater 39, 124–132. https://doi.org/10.1016/j.actbio.2016.05.011

Denora, N., Lopedota, A., Perrone, M., Laquintana, V., Iacobazzi, R.M., Milella, A., Fanizza, E., Depalo, N., Cutrignelli, A., Lopalco, A., Franco, M., 2016. Spray-dried mucoadhesives for intravesical drug delivery using N-acetylcysteine- and glutathione-glycol chitosan conjugates. Acta Biomater 43, 170–184. https://doi.org/10.1016/j.actbio.2016.07.025

Galluzzi, L., Buqué, A., Kepp, O., Zitvogel, L., Kroemer, G., 2017. Immunogenic cell death in cancer and infectious disease. Nat Rev Immunol 17, 97–111. https://doi.org/10.1038/nri.2016.107

Gentile, L., de Luca, G., Antunes, F.E., Rossi, C.O., Ranieri, G.A., 2010. Thermogelation analysis of F127-water mixtures by physical Chemistry techniques. Applied Rheology 20. https://doi.org/10.3933/ApplRheol-20-52081

Harris, R.E., 2007. and the Inflammogenesis of Cancer 2, 93–126.

Hayashi, K., Nikolos, F., Lee, Y.C., Jain, A., Tsouko, E., Gao, H., Kasabyan, A., Leung, H.E., Osipov, A., Jung, S.Y., Kurtova, A. v., Chan, K.S., 2020. Tipping the immunostimulatory and inhibitory DAMP balance to harness immunogenic cell death. Nat Commun 11, 1–13. https://doi.org/10.1038/s41467-020-19970-9

Hock, N., Racaniello, G.F., Aspinall, S., Denora, N., Khutoryanskiy, V. v., Bernkop-Schnürch, A., 2022. Thiolated Nanoparticles for Biomedical Applications: Mimicking the Workhorses of Our Body. Advanced Science 9, 1–24. https://doi.org/10.1002/advs.202102451

Ifshin, M.S., Johnson, K.E., Eaton, D.C., 1983. Membrane Biology Acid pH and Weak Acids Induce Na-Cl Cotransport in the Rabbit Urinary Bladder, J. Membrane Biol.

Lin, T., Wu, J., Zhao, X., Lian, H., Yuan, A., Tang, X., Zhao, S., Guo, H., Hu, Y., 2014. In situ floating hydrogel for intravesical delivery of adriamycin without blocking urinary tract. J Pharm Sci 103, 927–936. https://doi.org/10.1002/jps.23854

Lopedota, A., Cutrignelli, A., Laquintana, V., Denora, N., Iacobazzi, R.M., Perrone, M., Fanizza, E., Mastrodonato, M., Mentino, D., Lopalco, A., Depalo, N., Franco, M., 2016. Spray Dried Chitosan Microparticles for Intravesical Delivery of Celecoxib: Preparation and Characterization. Pharm Res 33, 2195–2208. https://doi.org/10.1007/s11095-016-1956-7

Mader, W.J., Higuchi, T., 1970. Phase Solubility Analysis. C R C Critical Reviews in Analytical Chemistry 1, 193–215. https://doi.org/10.1080/10408347008542734

Malanga, M., Szemán, J., Fenyvesi, É., Puskás, I., Csabai, K., Gyémánt, G., Fenyvesi, F., Szente, L., 2016. "Back to the Future": A New Look at Hydroxypropyl Beta-Cyclodextrins. J Pharm Sci 105, 2921–2931. https://doi.org/10.1016/j.xphs.2016.04.034

Mennini, N., Furlanetto, S., Cirri, M., Mura, P., 2012. Quality by design approach for developing chitosan-Ca-alginate microspheres for colon delivery of celecoxib-hydroxypropyl-β-cyclodextrin-PVP complex. European Journal of Pharmaceutics and Biopharmaceutics 80, 67–75. https://doi.org/10.1016/j.ejpb.2011.08.002

Morita, Y., Hata, K., Nakanishi, M., Nishisho, T., Yura, Y., Yoneda, T., 2012. Cyclooxygenase-2 promotes tumor lymphangiogenesis and lymph node metastasis in oral squamous cell carcinoma. Int J Oncol 41, 885–892. https://doi.org/10.3892/ijo.2012.1529

Nagarsenker, M.S., Joshi, M.S., 2005. Celecoxib-cyclodextrin systems: Characterization and evaluation of in vitro and in vivo advantage. Drug Dev Ind Pharm 31, 169–178. https://doi.org/10.1081/DDC-200047795

Perrone, M., Lopalco, A., Lopedota, A., Cutrignelli, A., Laquintana, V., Franco, M., Bernkop-Schnürch, A., Denora, N., 2018. S-preactivated thiolated glycol chitosan useful to combine mucoadhesion and drug delivery. European Journal of Pharmaceutics and Biopharmaceutics 132, 103–111. https://doi.org/10.1016/j.ejpb.2018.09.015

Pistone, M., Racaniello, G.F., Arduino, I., Laquintana, V., Lopalco, A., Cutrignelli, A., Rizzi, R., Franco, M., Lopedota, A., Denora, N., 2022. Direct cyclodextrin-based powder extrusion 3D printing for one-step production of the BCS class II model drug niclosamide. Drug Deliv Transl Res 12, 1895–1910. https://doi.org/10.1007/s13346-022-01124-7

Racaniello, G.F., Laquintana, V., Summonte, S., Lopedota, A., Cutrignelli, A., Lopalco, A., Franco, M., Bernkop-Schnürch, A., Denora, N., 2021. Spray-dried mucoadhesive microparticles based on S-

protected thiolated hydroxypropyl-β-cyclodextrin for budesonide nasal delivery. Int J Pharm 603, 120728. https://doi.org/10.1016/j.ijpharm.2021.120728

Raghavan, S.R., Cipriano, B.H., 2006. Gel formation: Phase diagrams using tabletop rheology and calorimetry. Molecular Gels: Materials with Self-Assembled Fibrillar Networks 241–252. https://doi.org/10.1007/1-4020-3689-2_9

Ramaiah Chowdary, K.P., Srinivas, S.V., 2006. Influence of hydrophilic polymers on celecoxib complexation with hydroxypropyl β-cyclodextrin. AAPS PharmSciTech 7, 3–8. https://doi.org/10.1208/pt070379

Ramirez, D., Gupta, A., Canter, D., Harrow, B., Dobbs, R.W., Kucherov, V., Mueller, E., Streeper, N., Uhlman, M.A., Svatek, R.S., Messing, E.M., Lotan, Y., 2016. Microscopic haematuria at time of diagnosis is associated with lower disease stage in patients with newly diagnosed bladder cancer. BJU Int 117, 783–786. https://doi.org/10.1111/bju.13345

Ricci, F., Racaniello, G.F., Lopedota, A., Laquintana, V., Arduino, I., Lopalco, A., Cutrignelli, A., Franco, M., Sigurdsson, H.H., Denora, N., 2022. Chitosan/sulfobutylether-β-cyclodextrin based nanoparticles coated with thiolated hyaluronic acid for indomethacin ophthalmic delivery. Int J Pharm 622. https://doi.org/10.1016/j.ijpharm.2022.121905

Sanli, O., Dobruch, J., Knowles, M.A., Burger, M., Alemozaffar, M., Nielsen, M.E., Lotan, Y., 2017. Bladder cancer. Nat Rev Dis Primers 3, 1–19. https://doi.org/10.1038/nrdp.2017.22

Schuetz, Y.B., Gurny, R., Jordan, O., 2008. A novel thermoresponsive hydrogel based on chitosan. European Journal of Pharmaceutics and Biopharmaceutics 68, 19–25. https://doi.org/10.1016/j.ejpb.2007.06.020

Şenyiğit, Z.A., Karavana, S.Y., İlem-Özdemir, D.I., Çalışkan, C., Waldner, C., Şen, S., Bernkop-Schnürch, A., Baloğlu, E., 2015. Design and evaluation of an intravesical delivery system for superficial bladder cancer: Preparation of gemcitabine HCl-loaded chitosan-thioglycolic acid nanoparticles and comparison of chitosan/poloxamer gels as carriers. Int J Nanomedicine 10, 6493–6507. https://doi.org/10.2147/IJN.S93750

Sherif, A.Y., Mahrous, G.M., Alanazi, F.K., 2018. Novel in-situ gel for intravesical administration of ketorolac. Saudi Pharmaceutical Journal 26, 845–851. https://doi.org/10.1016/j.jsps.2018.03.014

Shriky, B., Kelly, A., Isreb, M., Babenko, M., Mahmoudi, N., Rogers, S., Shebanova, O., Snow, T., Gough, T., 2020. Pluronic F127 thermosensitive injectable smart hydrogels for controlled drug delivery system development. J Colloid Interface Sci 565, 119–130. https://doi.org/10.1016/j.jcis.2019.12.096

Simões, S.M.N., Veiga, F., Torres-Labandeira, J.J., Ribeiro, A.C.F., Sandez-Macho, M.I., Concheiro, A., Alvarez-Lorenzo, C., 2012. Syringeable Pluronic-α-cyclodextrin supramolecular gels for sustained delivery of vancomycin. European Journal of Pharmaceutics and Biopharmaceutics 80, 103–112. https://doi.org/10.1016/j.ejpb.2011.09.017

Sinha, V.R., Nanda, A., Chadha, R., Goel, H., 2011. Molecular simulation of hydroxypropyl-β-cyclodextrin with hydrophobic selective COX-II chemopreventive agent using host-guest phenomena. Acta Poloniae Pharmaceutica - Drug Research 68, 585–592.

Tutak, A.Ş., Findikli, H.A., 2021. Could urine pH be a new parameter for mortality? Progress in Nutrition 23. https://doi.org/10.23751/pn.v23i2.11626

van Rhijn, B.W.G., Burger, M., Lotan, Y., Solsona, E., Stief, C.G., Sylvester, R.J., Witjes, J.A., Zlotta, A.R., 2009. Recurrence and Progression of Disease in Non-Muscle-Invasive Bladder Cancer: From Epidemiology to Treatment Strategy. Eur Urol 56, 430–442. https://doi.org/10.1016/j.eururo.2009.06.028

Yoon, H.Y., Yang, H.M., Kim, C.H., Goo, Y.T., Kang, M.J., Lee, S., Choi, Y.W., 2020. Current status of the development of intravesical drug delivery systems for the treatment of bladder cancer. Expert Opin Drug Deliv 17, 1555–1572. https://doi.org/10.1080/17425247.2020.1810016